

# On the ground states of an array of magnetic dots in the vortex state and subject to a normal magnetic field.

J.E.L.Bishop

*Department of Physics and Astronomy, The University of Sheffield, Sheffield S3 7RH, U.K.*

A.Yu.Galkin

*Institute of Metal Physics, National Academy of Sciences of Ukraine, Vernadskii av. 36, 03142, Kiev, Ukraine*

B.A.Ivanov\*

*Institute of Magnetism, National Academy of Sciences of Ukraine, Vernadskii av. 36 "B", 03142, Kiev, Ukraine*

(Dated: November 5, 2018)

Dipole-dipole interactions in a square planar array of sub-micron magnetic disks (magnetic dots) have been studied theoretically. Under a normal magnetic field the ground-state of the array undergoes many structural transitions between the limiting chessboard antiferromagnetic state at zero field and the ferromagnet at a threshold field. At intermediate fields, numerous ferrimagnetic states having mean magnetic moments between zero and that of the ferromagnetic state are favorable energetically. The structures and energies of a selection of states are calculated and plotted, as are the fields required to optimally reverse the magnetic moment of a single dot within them. Approximate formulae for the dipolar energy and anhysteretic magnetization curve are presented.

## I. INTRODUCTION

Recently some peculiar properties of sub-micron magnetic particles (magnetic dots) fabricated from such soft magnetic materials as permalloy, Co, etc., and forming an artificial lattice have attracted great attention, see Refs. 1-5. These magnetic dot arrays constitute promising material for high-density magnetic storage media. The distribution of magnetization within the dots is quite non-trivial. In the absence of an external magnetic field, a small enough non-ellipsoidal dot exhibits a single-domain nearly uniform magnetization state, either a so called flower state or a leaf state.<sup>6</sup> On increasing the size of the dot above a critical value, a vortex state occurs.<sup>7</sup> This vortex state has been experimentally observed ( see Refs. 4, 5, 8 - 10) for circular disk-shaped magnetic dots with diameters  $2R = 200 - 800$  nm and thickness  $L = 20 - 60$  nm. In Ref. 11, magnetization reversal for an array of disk-shaped dots under the influence of a magnetic field applied in the plane of the dots has been investigated experimentally. In this planar geometry the main contribution to the total magnetization comes from the internal reorganization of each dot's magnetic structure, in particular, by displacement of the vortex from the dot center, leading eventually to annihilation of the vortex at the rim of the dot. In this process, dipolar interaction between the dots does not play an essential role.

In the present work, another case, namely, the ground state of an unbounded planar square lattice of thin circular disk-shaped dots in an external magnetic field perpendicular to the plane of the dots will be considered. We will show that the situation in this case is very different from that in which the field is applied in-plane: the main contribution to the total magnetization is now determined as much by the dipolar interactions of the dots as by the external field. In a perpendicular field, the

dipole-dipole interaction between the dots results in a complex specific phase diagram. In particular, a cascade of phases with different patterns of dot magnetization has been found; these constitute the sequence of ground states as a function of the external magnetic field.

## II. MODEL

In order to formulate the model we need to discuss briefly the character of  $\vec{M}$ , the magnetization distribution within a single dot in the vortex state. In circular cylindrical coordinates,  $\vec{M} = \vec{M}(z, r, \chi)$ . In sufficiently thin material, such as that being considered in the present work,  $\vec{M}$  does not depend significantly on the  $z$ -coordinate along the normal to the dot, so that we may more simply write  $\vec{M} = \vec{M}(r, \chi)$ , where  $r$  and  $\chi$  are the polar coordinates in the dot plane. Then the Cartesian components of  $\vec{M}$  for the vortex state inside the dot,  $M_x = M_s \sin \theta \cos \varphi$ ,  $M_y = M_s \sin \theta \sin \varphi$ ,  $M_z = M_s \cos \theta$ , where  $M_s$  is the saturation magnetization, are determined by ansatz

$$\theta = \theta(r), \varphi = \chi + \varphi_0. \quad (1)$$

Such a distribution is typical for magnetic vortices with a topological charge (vorticity) equal to one, in two-dimensional easy-plane ferromagnets. The function  $\theta(r)$  is determined by an ordinary differential equation and its solution can be easily found numerically – see the general discussion of magnetic vortices in Refs. 12, 13.

For the theory of magnetic dots made of soft magnetic materials, the crystallographic easy-plane anisotropy is negligible, and the demagnetizing field  $\vec{H}_m$  plays the main role. The sources of  $\vec{H}_m$  are both the volume

"magnetic charges", proportional to  $\text{div}\vec{M}$ , and the discontinuity in the normal component of magnetization at the surface of the sample (the surface "magnetic charges"). The vortex distribution (1) has an advantage compared with others, because for (1)  $\text{div}\vec{M} = M_s \cos\varphi_0 \left( \frac{d\theta}{dr} \cos\theta + \frac{1}{r} \sin\theta \right)$ , and  $\text{div}\vec{M} = 0$  at  $\varphi_0 = \pm\pi/2$ . Accordingly, the volume magnetic charges vanish and the sole source of the field is the  $z$ -projection of  $\vec{H}_m$  onto the faces of the dot. The states with  $\varphi_0 = +\pi/2$  and  $\varphi_0 = -\pi/2$  have the same energy, i.e. the vortex state of the dot is twofold degenerate with respect to the sense of the magnetization rotation. In the case of a thin enough dot, this gives  $\vec{H}_m = -4\pi M_s \hat{z}$ , i.e. there is an effective easy plane anisotropy  $w_m = 2\pi M_s^2 \cos^2\theta$ .

The function  $\theta(r)$  can be obtained by applying well-known methods for treating magnetic vortices in easy plane magnets. In the center of the dot ( $r = 0$ ) the function  $\theta(r)$  is restricted to two possible values  $\theta(r = 0) = 0, \pi$ ; so that  $\cos\theta = p = \pm 1$ . Here  $p$  is the so-called vortex polarization (the second topological charge).<sup>13</sup> The characteristic scale of the variation of the function  $\theta(r)$  coincides with the value of the exchange length  $\Delta_0$

$$\Delta_0 = \sqrt{A/4\pi M_s^2}, \quad (2)$$

where  $A$  is the inhomogeneous exchange constant.

For  $r \gg \Delta_0$  in the vortex solution, the value  $\theta(r)$  tends to  $\pi/2$  exponentially. If the dot radius  $R \gg \Delta_0$ , then one can obtain an acceptable solution in which the limiting value  $\theta(r) = \pi/2$  is reached at  $r = R$ , the rim of the dot. In this case  $\theta \approx \pi/2$  within the major part of the volume of the dot, where  $\Delta_0 < r \leq R$ . Such states have been discussed in a theoretical treatment of magnetic dots that included an exact treatment of the magnetic dipole-dipole interaction.<sup>7</sup> That treatment showed that the out-of-plane magnetization  $M_z$  is significantly different from zero only in the core region,  $r \leq \Delta_0$ , and that the total magnetic moment of the dot  $\vec{\mu}$  has one of two values:

$$\vec{\mu} = p\mu\hat{z}, p = \pm 1, \mu = 2\pi\xi L\Delta_0^2 M_s, \quad (3)$$

where  $\xi$  is a multiplicative constant of the order of 1; in fact  $\xi \rightarrow 1.361$  as  $\Delta_0/R \rightarrow 0$ .

Thus, we arrive at the following simplified picture of the state of the single dot. In the greater part of the dot, the magnetization lies in the dot plane, rotating about the center of the dot, and so, because of its circular symmetry, does not contribute to the total moment  $\vec{\mu}$  of the dot.<sup>7</sup> The state of the dot is fourfold degenerate, with  $\varphi_0 = \pm\pi/2$  and the core polarization  $p = \pm 1$ . The value of  $\varphi_0$  does not manifest itself in the magnetic moment of the dot and, as a consequence, has no influence on dot interactions. The magnetic moment is directed perpendicular to the plane of the dot and has either of the values  $\pm\mu\hat{z}$ .

With regard to dot interactions, all dots are in one or other of two states: "up" and "down". Since the core volume is much smaller than the dot volume, the core magnetic moment is small compared with the saturation moment of the dot. Although the dipolar interaction between dots is not very strong,<sup>14</sup> it is nevertheless the sole source of interaction within the dot system. Because both the dipolar dot interaction field and the external magnetic field are very much lower than the effective fields (exchange and demagnetizing) internal to the dot, one can regard the magnetization distribution inside the dot as practically unaffected by them.

An important consequence of this robustness of the vortex state is that the polarization  $p$  and moment  $\vec{\mu}$  of a dot remain unchanged under the application of small enough external magnetic fields  $\vec{H}_e$  parallel to  $\hat{z}$ .<sup>15</sup> It is clear that not only the state with  $\vec{H}_e \parallel \vec{\mu}$  (light vortex) is stable, but also the state  $\vec{H}_e$  with antiparallel to  $\hat{z}$  (heavy vortex) remains constant and metastable up to  $|\vec{H}_e| = 4\pi M_s$ .<sup>15</sup>

Following from the above discussion, the Hamiltonian of a dot array can be presented as follows:

$$\mathcal{H} = \frac{\mu^2}{2a^3} \sum_{\vec{l} \neq \vec{l}'} \frac{p_{\vec{l}} p_{\vec{l}'}}{|\vec{l} - \vec{l}'|^3} - \mu H \sum_{\vec{l}} p_{\vec{l}}, \quad (4)$$

where  $\mu$  is the moment of a single dot,  $p_{\vec{l}} = \pm 1$ ,  $\vec{l}, \vec{l}'$  are dot positions in a square lattice,  $\vec{l} = a(m\hat{x} + n\hat{y})$ ,  $m, n = 0, \pm 1, \pm 2, \dots$  are integers,  $a$  is the interdot distance, and  $H$  is the external magnetic field parallel to  $\hat{z}$ . The first term describes the dipole-dipole interaction of the lattice of magnetic dots, the second term is the Zeeman energy.

It should, perhaps, be stressed that the system modelled here, consisting of a square lattice of discrete dipoles, normal to the lattice plane, with only dipolar interactions, is very different from a continuous thin film with perpendicular anisotropy. Numerical treatments of such films, when performed using a square lattice discretization, eg. see Refs. 16, 17, give rise to a Hamiltonian that bears a superficial resemblance to that of the present system, but the essential continuity of the film, expressed in the exchange coupling between nearest neighbour elements of the numerical discretization - the dominant interaction in any sufficiently refined discretization - necessarily results in magnetization patterns (stripe domain structures) that are entirely different from the patterns of discrete moments arising from pure dipolar interactions between discrete dots on a square lattice that are reported here.

### III. MAGNETIC GROUND STATES

The dipole-dipole interaction is long-range, and it is not obvious *a priori* what structure will constitute the

ground state. For a system of particles with dipole-dipole interactions and in zero applied field, a theorem states that in the ground state the overall magnetic moment is zero, and this results in a specific antiferromagnetic (AFM) state.<sup>18</sup> For instance, in the case of a three-dimensional simple cubic lattice of spherical particles, a four-sub-lattice structure with non-collinear magnetic moments is optimal.<sup>19</sup> This is possible, however, only if the magnetic moment of each particle is free to point in any direction. Here, because of the robustness of the vortex state supporting the dot magnetic moment, we have  $p = \pm 1$  and uniaxial, giving rise to a quasi-Ising model. Determination of the ground state is reduced to geometrical considerations.

It is convenient to divide the initial simple square lattice, on which the dots are located, into elementary *magnetic* cells of rectangular shape with  $(k \times l)$  dots, so that the overall spatial arrangement of up and down ( $p = \pm 1$ ) dots (what we call their "structure", "configuration" or "pattern") can be produced from a single such cell by a translation  $\vec{T} = a(N\hat{x} + M\hat{y})$ , where  $M = km$  and  $N = ln$  and  $m, n = 0, \pm 1, \pm 2, \dots$  are integers. This is appropriate for a magnetic structure with sublattice number (i.e. smallest rectangular unit cell size) less than or equal to  $k \times l$ . Note that as the choice of specific values for  $k$  and  $l$  restricts the range of structures that can be represented in this way, the search for the ground state must, in principle, extend to all integer  $k, l$ . The Zeeman energy, however, depends only on the relative numbers of dots with  $p = +1$  and  $p = -1$  in a magnetic cell, i.e. on the mean moment per dot  $\langle \mu \rangle (= \langle \mu_z \rangle)$ , and, of course, on the applied field  $H$ .

We have investigated a substantial number of states, namely, all states with  $k \times l = 2, 3$  and  $4$ , and many states with larger values of  $k$  and  $l$ . Because the dipolar interaction falls off with the inverse cube of the moment separation, i.e. quite rapidly, it is clear that distributions in which dots of like orientation are well apart from each other, while those of opposite sign are as close as possible, will be energetically most favourable. In particular, one notes that the ratio of the interaction energy of a nearest neighbour dot pair, to that of a pair of next-nearest neighbours, is  $\sqrt{8} : 1$ . It seems extremely improbable that two dots of the minority population (which we will consistently take to be the down dots with  $p = -1$ ) could ever be nearest neighbours in a ground-state configuration. In zero magnetic field, the most energetically favorable distribution is the simple chessboard AFM structure, see Fig. 1. In this structure neither of the two (equal) populations contains any nearest neighbour pairs of parallel dots. Other AFM structures in which dots with the same value of  $\vec{\mu}$  do occur as nearest neighbours possess very much higher energy as is illustrated by the examples in Fig. 1.

For the AFM structure, the energy does not depend on the applied magnetic field, whereas for the ferromagnetic (FM) structure (with  $\vec{\mu} = +\mu\hat{z}$  for all dots) this dependence is maximal. The total mean energy per dot can

be written as  $W = W_m - \langle \mu \rangle H$ , where  $W_m$  is the mean energy, per dot, of the dipole-dipole interaction and  $\langle \mu \rangle$  is the overall average moment per dot of the distribution (zero in the AFM case). In virtue of this, the energies  $W_{FM}$  and  $W_{AFM}$  of the FM and AFM states, for which  $W_m = W_{FM}, W_{AFM}$  respectively, become equal at some field  $H^* = 2(W_{FM} - W_{AFM})/\mu$ , and, if these were the only states possible, one could expect a first order phase transition from the AFM to the FM structure at  $H = H^*$ . However, numerous other states are possible, and the situation is very much more complicated.

In the intermediate region between AFM and FM, numerous more complex structures with  $0 < \langle \mu \rangle < \mu$  ("ferrimagnetic" structures) may occur. For these states, the dipole-dipole interaction energy,  $W_m$ , is higher than  $W_{AFM}$ , that for the optimal chess AFM, but the total energy  $W_{m,H} = W_m - \langle \mu \rangle H$  is reduced with increasing field  $H$ . Therefore, such structures may constitute the ground state at finite magnetic fields. To describe these structures, it is convenient to introduce the dimensionless magnetization  $m = \langle \mu \rangle / \mu$ .

In order to determine the values of  $H$  that fix the lower and upper bounds of such ferrimagnetic ground states, we have calculated the change in dipole-dipole interaction energy  $\Delta W_m$  that occurs when the magnetic moment of a single dot is reversed in the FM and chessboard AFM structures. A simple analysis shows that this energy change is determined by the energy per dot in the initial states. Reversing the magnetic moment of one dot in the FM state requires  $\Delta W_m = 4W_{FM}$ , and in the chessboard AFM state  $\Delta W_m = 4|W_{AFM}|$ . The value of  $W_{FM}$  found numerically is  $4.516811\mu^2/a^3$ . Including the magnetic field, one can show that the total energy  $W_{FM}$  of the pure FM state and that of the same state, but with one dot reversed, coincide at the value  $H = H_1$ , where

$$H_1 = 2W_{FM}/\mu = 9.033622 \mu/a^3. \quad (5)$$

Evidently, for  $H > H_1$  the FM structure is the most favorable, but with  $H < H_1$ , some magnetic moments tend to reverse. When  $H < H_1$ , but close to  $H_1$ , the density of these reversed moments will be very low and  $\langle \mu \rangle \approx \mu$ .

The chessboard AFM state can be treated in the same way. One obtains  $W_{AFM} = -1.322943\mu^2/a^3$  and for the corresponding threshold field  $H_0$ , above which it becomes favorable to switch a dot from antiparallel to parallel to the field direction, one finds  $H_0 = 2|W_{AFM}|/\mu = 2.645886 \mu/a^3$ .

Hence, intermediate phases with  $0 < \langle \mu \rangle < \mu$  exist within the finite range of fields,  $H_0 < H < H_1$ , and  $\langle \mu \rangle \rightarrow 0$  as  $H \rightarrow H_0$ , and  $\langle \mu \rangle \rightarrow 1$  as  $H \rightarrow H_1$ . Let us consider the nature of the ground states in this field range. In the limit of low fields, these states are obtained from the chessboard AFM by reversing the magnetic moments of a small fraction of the down dot population, leaving the remainder undisturbed. At high fields  $H \approx H_1$ , the initial structure is the FM one. In both

cases, one expects the flipped dots to be dispersed as far from each other as possible, in order to minimize their contribution to the dipole-dipole interaction energy of the system. If it were not for the constraints imposed by the square lattice on which all the dots are located, one would therefore expect these flipped dots to lie on an equilateral triangular lattice.

Guided by these considerations, we have sought and found excellent candidates for those configurations for which  $W_m$  is minimal, for a number of fixed values of  $m = \langle \mu \rangle / \mu$  between 0 and 1. The elementary rectangular magnetic cells that represent a selection of these "optimal" (we drop the parentheses hereafter) configurations are depicted in Figs. 2 and 3, together with their corresponding values of  $m$  and  $W_m$  (with  $W_m$  expressed in units of  $\mu^2/a^3$ ). These  $W_m$  (also the values for  $W_{FM}$  and  $W_{AFM}$  given above) were evaluated numerically by summing the contributions to the field, at each dot in the cell, of all dots within a radius  $10,000.5a$ . The contribution from all more distant dots was approximated by attributing a uniform areal dipolar moment density  $m\mu/a^2$  to the area of the plane of the dots outside that radius. All values of  $W_m$  obtained in this way are plotted as the points in Fig. 4.

The sequence of configurations in Figs. 2 and 3 represent some of the (very many) stages in the anhysteretic magnetization of the dot array from the demagnetized AFM to the fully magnetized FM state. Owing to the stability of the vortex state in the dots, it is evident that these states probably cannot be accessed sequentially merely by increasing the applied field. They represent stages in an *ideal* anhysteretic sequence, probably accessible only by thermal, or quasi-thermal (e.g. magnetic "shaking") cooling through the Curie temperature (or quasi-Curie temperature), under the appropriate constant normal magnetic field  $H(m)$ .

It is also evident that the configurations reported here constitute only a small sample drawn from an infinite sequence of such optimal configurations over the range  $0 \leq m < 1$ : for every rational value of  $m$  in this range, there exist, in principle, numerous different configurations, one (or possibly more) of which must possess the lowest value of  $W_m$ . (Henceforward, unless the contrary is explicit,  $W_m$  will be used exclusively to refer to this lowest energy for given  $m$ .)

Less evident, but at least extremely plausible, is the hypothesis that  $W_m$  increases monotonically with  $m$ . Consider the optimal configurational state, in zero applied field, for any specific reduced magnetization  $m$ . In both the majority "up" dot and minority "down" dot populations, the dots are occupying the "energetically best" locations available to them. However, by virtue of being in the minority population, even the least favorably located of the "down" dots is surely more favorably located than the least favorably located "up" dot: it has more dots of opposite sign with which to interact, and need have no dot of the same sign for a nearest neighbour; the least favorably located "up" dot, by contrast, is certain to have

another "up" dot alongside. How, then can it be energetically favorable to reverse the moment of a "down" dot, thereby creating yet another "up" dot? Indeed, this argument can be pushed a stage further: not only must  $W_m$  increase monotonically with  $m$ , but so must its rate of increase,  $dW_m/dm$ , because the dots being reversed are selected in order of increasing stability and new sites for reversed dots are increasingly less favorable. It appears, however, that  $dW_m/dm$ , though monotonically increasing, is discontinuous. For example, consider a state with a simple structure like that for  $m = 1/2$  in Fig. 2. It is evident that the energy increase on reversing one of the minority down dots is substantially greater than the energy decrease on reversing one of the majority up dots (taking into account the decrease in the former energy change and increase in the latter on optimizing the two new states). Indeed we have carried out this procedure for all but one (that for  $m = 27/28$  which is very close to the FM state) of our optimal configuration candidates, all of which support this prediction. This aspect is further discussed in Section IV.

#### IV. ANALYTIC ASYMPTOTIC APPROXIMATIONS

Analytic formulae designed to approximate the dipolar energy  $W_m$  in the limits  $m \rightarrow 0$  and  $m \rightarrow \infty$  will now be derived. These formulae are both instructive and in remarkably good accord with the numerical values of  $W_m$  calculated for specific states and represented by the points plotted in Fig. 4.

##### A. Approximations near FM state

###### 1. Equilateral triangular superlattice

Consider states with  $m = 1 - \epsilon, 0 < \epsilon \ll 1$ . In this region, as mentioned earlier, one expects the minority down dots to be distributed as far from each other as possible, thereby minimizing their positive dipolar interactions with one another and maximizing their negative interactions with the majority up dots. For a given density of minority dots, as prescribed by  $\epsilon$ , their maximum separation is known to be ideally accomplished when those dots form an equilateral triangular lattice (ETL hereafter). In the present case this cannot be precisely achieved because all the dots are constrained to lie only at points on the fundamental square lattice of spacing  $a$ . However, when  $\epsilon$  is very small, the spacing of the minority dots  $\lambda \gg a$ , and they can adopt a fair approximation to an equilateral triangular distribution, and indeed, as  $\epsilon \rightarrow 0$ , this approximation will become very good. In developing our approximate formula, we will therefore assume the minority dots all lie on an ETL with spacing  $\lambda(\epsilon)$ .

In order to proceed, we need to know the interaction field and energy for dots in an FM state on an ETL. This was calculated numerically, in a manner similar to that used for distributions on a square lattice described above, again summing over a circular region, of radius  $R = 10000.5\lambda$ , surrounding a central dot at which the field of the others is calculated. At lattice spacing  $\lambda$ , there are  $(2/\sqrt{3})/\lambda^2$  dots per unit area. The region outside  $R$  was represented, as before, as uniformly polarized with the mean dipole moment per unit area,  $(2/\sqrt{3})\mu/\lambda^2$ . The numerical calculation yields an energy per dot  $W_{FM\Delta} = 5.517088 \mu^2/a^3$ . For  $\lambda = a$ ,  $W_{FM\Delta}$  is substantially higher than the value  $W_{FM} = 4.516811 \mu^2/a^3$  obtained for the square lattice, but that is because the dot areal density is a factor  $2/\sqrt{3}$  higher. For the same dot areal density,  $1/a^2$ , we require  $\lambda = [2/\sqrt{3}]^{1/2}a$ . Because of the inverse cube interaction law, the energy per dot, at the same dot density,  $1/a^2$ , is a factor  $[(\sqrt{3})/2]^{3/2}$  lower than  $5.517088 \mu^2/a^3$ . This gives  $W_{FM\Delta} = 4.446373 \mu^2/a^3$  for an ETL of moment density  $\mu/a^2$ , about 1.56% lower than  $W_{FM}$  for the square lattice, demonstrating the small but significant energetic advantage of the former configuration. (Indeed, the smallness of this energy difference, for such very different configurations, is reassuring, for it indicates that the small departures from the ideal ETL, that are imposed by conformity with the underlying square lattice, will not introduce any substantial error.) Analogous to  $H_1 = 2W_{FM}/\mu = 9.033622 \mu/a^3$ , we will write  $H_\Delta = 2W_{FM\Delta}/\mu = 8.8927451 \mu/a^3$ . The self-energy per dot, of an ETL of dots, with moment  $\mu$  per dot, and dot areal density  $(\epsilon/2a^2)$ , is  $(\epsilon/2)^{3/2}W_{FM\Delta}$  in the FM state. Returning to the  $m = 1 - \epsilon$  system, we can regard it as the *superposition*, on the uniform square FM dot lattice, of an (approximately) equilateral triangular system of "double-dots" of moment  $-2\mu$  and of moment areal density  $-\epsilon\mu/a^2$ , i.e. with spacing  $\lambda = [(2/\sqrt{3})(\epsilon/2)]^{1/2}a$  appropriate to a dot areal density  $-\epsilon/2a^2$ . We superpose double-dots in order, in effect, to *reverse* the moments  $\mu$  of that fraction,  $\epsilon/2$ , of dots on the basic square lattice that constitute the (approximate) ETL of up dots that require to be reversed to achieve the required overall reduced moment  $m = 1 - \epsilon$ . The contribution to the energy of each double-dot, of moment  $-2\mu$ , due to its interaction with all the other double-dots, is  $4W_{FM\Delta}(\epsilon/2)^{3/2}$ . This contributes  $4(\mu H_\Delta/2)(\epsilon/2)^{5/2}$  to the mean dipolar energy per dot of the overall square lattice, in this analytic asymptotic approximation for  $m \approx 1$ , denoted  $W_{a1}$ . In addition, the double-dots also experience the field  $-H_1$  of the underlying square FM lattice on whose dots they are superimposed. Consequently the interaction energy of the triangular and square lattices is  $-\mu\epsilon H_1$ , per square lattice dot. The self-energy of the square FM lattice is, of course, just  $W_{FM} = \mu H_1/2$  per dot. Adding the three contributions gives for the mean energy per dot of the  $m = 1 - \epsilon$  system:

$$W_{a1} = \mu H_1(0.5 - \epsilon) + 4(\mu H_\Delta/2)(\epsilon/2)^{5/2}. \quad (6)$$

This formula is represented by the curve  $W_{a1}(m)$  that extends from  $m = 0.5$  to  $m = 1$  in Fig. 4. Agreement with the points  $W$  that represent the numerical values calculated for specific optimal structures is remarkably good, not only near  $m = 1$ , but over the whole of this range. One notes also that over the whole range, the approximate values  $W_{a1} \leq W_m$ , the "exact" numerical values for specific configurations. This is as it should be, because, in the approximation, the minority dots are located on an *ideal* ETL whereas, in the configurations treated numerically, the minority dots are restricted to points on the square lattice that are close to, but not precisely at, the ideal locations.

## 2. Square superlattice

Examination of the specific configurations treated numerically and illustrated in Fig. 3 reveals that, in some cases, notably those for  $m = 3/5$  and  $m = 4/5$ , the requirement that all dots lie on the basic square lattice is so restrictive that the minority dots are obliged to lie on a square superlattice, no better approximation to the ideal ETL being available. It is instructive therefore to modify the above treatment and adapt it to a square lattice. Whereas the minority dots can only ever approximately conform to an ETL, they can lie precisely on a square lattice whenever the area per minority dot is  $k^2 + l^2$  with  $k, l$  integers. Of the three contributions to the mean energy per dot expressed in Eq. (6), only the self-energy of the double-dot lattice requires modification: in place of  $H_\Delta$  in that equation, we require  $H_1$ . Or, expressed rather in terms of  $W_{FM} = 0.5\mu H_1$ , we obtain for the energy per dot of the system with minority dots on a square superlattice:

$$W_\square = W_{FM}[1 - 2\epsilon + 4(\epsilon/2)^{5/2}]. \quad (7)$$

This expression yields precisely the same values as those found directly numerically for the specific structures proposed for  $m = 3/5$  and  $m = 4/5$  in Fig. 3 and also, for  $m = 0$ , that quoted above for  $W_{AFM}$ . We have  $W_{AFM} = W_{FM}[(1/\sqrt{2}) - 1]$ .

Because  $H_\Delta$  and  $H_1$  differ by only 1.56% and the double-dot lattice self-energy term is proportional to  $\epsilon^{5/2}$ ,  $W_\square$  differs very little from  $W_{a1}$  over the range  $1/2 \leq m \leq 1$ ; the difference in the worst case,  $m = 1/2$ , is only 1.11%. We do not include a curve representing  $W_\square$  in Fig. 4 because it can scarcely be distinguished from that for  $W_{a1}$ . Over the range  $1/2 \leq m \leq 1$ , whereas  $W_{a1}$  represents a close underestimate of  $W_m$ ,  $W_\square$  provides a similarly close overestimate.

## B. Approximation near AFM state

Here we consider states with positive  $m$  close to 0. The treatment resembles that in the environs of the FM

state discussed above. We again expect the dots that depart from the chessboard AFM structure ("up" dots this time), to be distributed as far from each other as possible, in locations approximating an ETL. Again we assume these "exceptional" dots all lie on an *ideal* ETL with spacing  $\lambda$ , and replace  $\epsilon$  in the above discussion of the triangular lattice energy by  $m$ . We now superpose the triangular lattice of "double-dots" on the AFM lattice instead of the FM one, an important difference being that we must, of course, place the positive double-dots only on top of negative dots of the underlying AFM lattice, whereas all dots in the FM lattice were equivalent and available for reversal.

Apart from the replacement of  $\epsilon$  by  $m$ , the expression for the self-energy of the double-dot triangular lattice is the same:  $4(\mu H_\Delta/2)(m/2)^{5/2}$  per dot of the overall square lattice. However, the interaction energy of the triangular and square lattices is now positive,  $+m\mu H_0$  (as against  $-\epsilon\mu H_1$ ) per dot of the square lattice and the self-energy of the square AFM lattice is  $-\mu H_0/2$  per dot. Adding the three contributions gives for the mean energy per dot of the overall lattice of weak reduced magnetization  $m$ :

$$W_{a0} = \mu H_0(m - 0.5) + 4\mu(H_\Delta/2)(m/2)^{5/2}. \quad (8)$$

Note that the two asymptotic approximations  $W_{a0}$  and  $W_{a1}$  happen to coincide at  $m = 0.5$ . The expression for  $W_{a0}$  is represented by the curve  $W_{a0}(m)$  that extends from  $m = 0$  to  $m = 0.5$  in Fig. 4. Again, agreement with the points  $W$  that represent the numerical values calculated for specific optimal structures is remarkably good, not only near  $m = 0$ , but over the whole range  $0 \leq m \leq 0.5$ . However, the agreement is not quite as good as was the case for  $W_{a1}$ , very probably owing to the additional constraint that only dots from the down-dot population are available for reversal, whereas in the FM case, all dots were available. This makes it somewhat harder (in an actual configuration, but not, of course, in the analytic approximation) to arrange the non-AFM dots close to the ideal triangular lattice. This cannot, however be the only reason for the lower agreement because, whereas for the approximation near the FM state all  $W_{a1} \leq W_m$ , some  $W_{a0} > W_m$ . An outstanding example is that for  $m = 1/3$  where  $W_{a0} - W_m > 0.01\mu^2/a^3$ . The reason for this is that, in an actual configuration, the constraint, assumed in the analytic treatment for  $m < 0.5$ , that the ideal configuration is obtainable by reversing only some negative dots in the chessboard AFM configuration and without any further rearrangement of the structure, does not apply and, for values of  $m$  sufficiently higher than zero, a lower energy than  $W_{a0}$  can sometimes be achieved by violating this supposed constraint - see, for example, the simple configuration for  $m = 1/3$  in Fig. 2.

## V. ANHYSTERETIC MAGNETIZATION CURVE

Consider two optimal configurations, one of reduced magnetization  $m$ , the other of higher magnetization  $(m + \delta m)$ . Their energies in a normal magnetic field  $H$ ,  $W_{m,H} = W_m - m\mu H$  and  $W_{(m+\delta m),H} = W_{(m+\delta m)} - (m + \delta m)\mu H$ , will be equal only in the field  $H_{m,(m+\delta m)} = (W_{(m+\delta m)} - W_m)/(\mu\delta m)$ . In the limit  $\delta m \rightarrow 0$ , we obtain the following differential expression for the anhysteretic magnetization curve  $H_m(m)$ :

$$\mu H_m = dW_m/dm. \quad (9)$$

(Our remarks above concerning local discontinuities in  $dW_m/dm$  and its monotonic increase with  $m$  are clearly relevant here also to  $H_m$ .)

In Fig. 5 we have plotted points representing approximate values of  $H_m(m)$  derived from the numerical values of  $W_m$  calculated for our set of candidates for optimal configurations. They are labelled  $dW/dm$ , and represented by circles. These are approximations to  $H_m$  given by  $(W_{m(i+1)} - W_{m(i)})/\mu(m_{(i+1)} - m_{(i)})$  and plotted at the values  $m = (m_{(i+1)} + m_{(i)})/2$  located midway between successive configurations of the known set. (All fields are shown in units of  $\mu/a^3$ .)

Also plotted in Fig. 5, where they are labelled  $Ha1$  and  $Ha0$ , are smooth curves representing  $H_{a1}$  and  $H_{a0}$ , the analytic approximations to  $H_m$  obtained by differentiating the asymptotic equations (6) and (8) and dividing by  $\mu$ :

$$H_{a1} = -\mu^{-1}dW_{a1}/d\epsilon = H_1 - (5/2)H_\Delta(\epsilon/2)^{3/2}, \quad (10)$$

$$H_{a0} = \mu^{-1}dW_{a0}/dm = H_0 + (5/2)H_\Delta(m/2)^{3/2}. \quad (11)$$

(The corresponding equation for  $H_\square = -\mu^{-1}dW_\square/d\epsilon$  is not plotted in Fig. 5: it is practically indistinguishable from  $H_{a1}$  over the appropriate range  $0.5 \leq m \leq 1$ .) Both Equations (10) and (11) provide a good fit to  $dW_m/dm$  over their appropriate data ranges,  $0 \leq m \leq 0.5$  for  $H_{a0}$  and  $0.5 \leq m \leq 1$  for  $H_{a1}$ . As one would expect for such asymptotic approximations, the fits are best towards the limits  $m = 0$  and  $m = 1$ . Unlike the expressions (6) and (8), from which they are derived, equations (10) and (11) do not lead to coincident values at  $m = 0.5$ . That expressions (6) and (8) should yield the same value for  $W_m$  at  $m = 0.5$  is a remarkable coincidence; that their slopes  $dW_m/dm$  should also agree there, is scarcely to be expected! In fact the discontinuity between them is in remarkably good agreement with the corresponding step in the data for  $dW_m/dm$  in the vicinity of  $m = 0.5$ .

## VI. CONFIGURATIONAL STABILITY

The fields  $H_+(m)$  and  $H_-(m)$  required to render energetically favourable the reversal of a down or up dot

in the optimal configuration for any value of  $m$ , and the difference between them,  $H_+ - H_-$ , provide measures of the stability of that configuration. Limiting examples of these fields, for the AFM and FM states, namely  $H_0 \equiv H_+(m=0)$  and  $H_1 \equiv H_-(m=1)$ , were discussed earlier in this article. (In fact, the AFM state also has  $H_-(m=0) \equiv -H_0$ , so that it is stable over a wide field range,  $2H_0$ .) As mentioned earlier, we have determined numerically the extra energies  $\Delta W_{m+}$  and  $\Delta W_{m-}$  required to reverse a down dot or an up dot respectively (including local rearrangement of the resulting configurations to minimize their energy) in almost all our candidates for the optimal states of reduced magnetization  $m$ .

The values of the corresponding fields,  $H_{\pm}(m) = \Delta W_{m\pm}/2\mu$ , are plotted in Fig. 5. Some examples illustrating the local re-organization of the dot distributions after single-dot reversal are presented in Fig. 6. Intermediate values of  $m$  were selected for display in this figure because the patterns in that region are rather more complex and varied than those near  $m=0$  and  $m=1$  and usually give rise to greater ranges of field stability.

In Fig. 5 it is evident that a salient feature of the fields  $H_+$  and  $H_-$  in this intermediate range of magnetizations is indeed the very substantial width of the gap between them,  $H_+ - H_-$ , that defines the field range of stability of the pattern against single dot reversal. Towards the limits  $m=0$  and  $m=1$ , that gap shrinks towards zero. However, for the structure of the *pure* AFM state, *precisely* at  $m=0$ , the gap is at its widest:  $2H_0$ . ( $H_-$  for the pure AFM state is off-scale in Fig. 5) Throughout the range  $0 < m < 1$ , one expects  $H_+ > H_m > H_-$ , but, of course, we do not have values of  $H_m$  at the values of  $m$  that correspond precisely to the optimal configurations. However, one observes in Fig. 5 that, for almost every configuration (label  $i$ ),  $H_+(m_{(i)})$  exceeds the next value of  $H_m \approx (W_{m(i+1)} - W_{m(i)})/\mu(m_{(i+1)} - m_{(i)})$ , with  $m_{(i+1)} > m_{(i)}$ , while, in the reverse direction,  $H_-(m_{(i)}) < H_{m(i-1)}$ . This means that the field required to reverse a *single* down dot in one of our optimal configurations, even after allowing for local rearrangement of the pattern to minimize the increase in dipole-dipole interaction energy, usually exceeds the field required to render energetically favourable the reversal of the *infinite* array of down dots required to change (anhysteretically) the pattern to that of the optimal configuration appropriate to the next higher value of  $m$ . Similarly, to reverse a *single* up dot, also after local rearrangement, usually requires a reduction of the field to a value below that needed to favour the (anhysteretic) reversal of the *infinite* array of up dots needed to establish the optimal configuration for the next lower value of  $m$ .

Examples may be helpful here. Compare the central rectangles for the states  $m=1/2(+)$  and  $m=5/9$  in Fig. 6. The former has the lower mean reduced moment,  $13/24 < 5/9$ , and is embedded in an infinite array of even lower mean reduced moment,  $m=1/2$ , yet it requires a *higher* field,  $H_+(m=1/2) = 6.681 >$

$H_m(m=0.5277\dots) = 6.589$  (in  $\mu/a^3$  units), to equilibrate it with the  $m=1/2$  configuration than does the periodic  $m=5/9$  pattern. Likewise, compare the central rectangles for the states  $m=1/2$  and  $m=5/9(-)$  in Fig. 6. Both have the same mean reduced moment of  $1/2$ , but the  $m=5/9(-)$  rectangle is embedded in an infinite array of higher reduced moment,  $m=5/9$ , yet it requires a *lower* field,  $H_-(m=5/9) = 5.986 < H_m(m=0.5277\dots) = 6.589$  (in  $\mu/a^3$  units), to equilibrate it with that  $m=5/9$  configuration than does the periodic  $m=1/2$  pattern.

The reason for this *prima facie* somewhat paradoxical behaviour is that, when only a single dot is to be switched in an optimal regular periodic configuration, only very local rearrangement of the dot pattern can reduce the energy of the resulting perturbed system whose overall pattern, remote from the switched dot, must remain optimised for the original level of mean magnetization. It follows that the sequence of points constituting the ideal anhysteretic magnetization "curve" must correspond to a discontinuous sequence of stable energetically optimal dot configurations. Magnetization by monotonic variation of the applied field alone will exhibit very substantial hysteresis and will realize very few, if any, of the ideal magnetization patterns.

## VII. SUMMARY AND CONCLUSIONS

Unbounded two dimensional arrays of thin circular disk-shaped magnetic dots on a square lattice have been considered in the presence of a magnetic field perpendicular to the dot plane. The radii and thickness of the dots is such that a radially symmetric vortex magnetization structure is stable; at radii outside a relatively limited core, the magnetization lies almost in plane and parallel to the rim. The net moment  $\mu$  is due to the vortex core and is normal to the dot plane; it is practically unaffected by normal fields of magnitude comparable to those from other dots.

For every rational value of the reduced magnetization of the array,  $m = \langle \mu \rangle / \mu < 1$ , (ignoring sign) there exist very numerous possible arrangements of up and down dots, one (or more) of which must have minimum dipolar interaction energy  $W_m$ . We have calculated that energy for a range of excellent candidates for these ground states at various values of  $m$ , in particular those of the chessboard AFM state of  $m=0$  and the uniform FM state with  $m=1$ . We suggest and argue that, for the sequence of optimal configurations,  $W_m$  and  $dW_m/dm$  increase monotonically with  $m$ , and this is supported by our data in Fig. 4. ( $dW_m/dm$  is likely to be locally discontinuous). An analytic formula for  $W_m(m)$  is derived on the assumption that for  $m \rightarrow 1$ , the minority down dots are located near points on an equilateral triangular super-lattice. A similar formula is derived for  $m \rightarrow 0$  relating to the excess up dots. Remarkably, these formulae agree at  $m=1/2$  (though their gradients differ)

and fit the data for specific states very well, especially near  $m = 0$  and 1. A similar formula involving a square super-lattice instead of the triangular super-lattice gives results in precise agreement with the data for specific structures with  $m = 0, 0.6$  and  $0.8$ , these being those structures in which the minority dots do indeed lie on square super-lattices. It differs from the first asymptotic formula by little more than 1.11% over the appropriate range  $0.5 \leq m \leq 1$ .

Approximate data for the anhysteretic magnetization curve  $H_m(m) = \mu^{-1}(dW_m/dm)$  are derived from the data for specific states and compared with the predictions of the analytic formulae in Fig. 5. The agreement is good, particularly near  $m = 0$  and 1. The fields predicted by the two asymptotic formulae differ quite sharply at  $m = 1/2$ , where they indicate a step discontinuity in field that matches a similar step in  $H_m(m)$ , the data from the series of specific states.

The stability of the optimal configurations found was explored by determining the minimum field  $H_+$  required to reverse a single down dot and likewise the maximum field  $H_-$  at which a single up dot would reverse, assuming in both cases local reorganization of the resulting dot pattern to minimize its energy. The gap  $H_+ - H_-$  between the two fields that indicates the stability of the configuration increases irregularly from near zero, for  $m$  just greater than zero, to a rough maximum around  $m = 1/2$  and then decreases again towards zero at  $m = 1$ . An exception to this general trend is the very large value at  $m = 0$  where  $H_+ = -H_- = H_0$ . For the optimal configurations at most values of  $m$ ,  $H_+ > H_{m+}$ , and  $H_- < H_{m-}$ , where  $H_{m+}$  and  $H_{m-}$ , refer to the optimal configurations studied at neighbouring values of magnetization, just above and just below  $m$ . It follows that there exists, with increasing  $m$ , a sequence of stable optimal configurations with energy barriers between them. It must be stressed, therefore, that the field curve  $H_m(m)$  is strictly an ideal *anhysteretic* magnetization curve: owing to the stability of the individual dot moments, the

individual dot distributions are likewise very stable, and the infinite sequence of energetic optimal states cannot be traced experimentally by monotonically increasing (or decreasing) the normal field alone. To realize any specific state it would be necessary - but perhaps not sufficient - to cool the sample through the Curie temperature subject to a normal magnetic field of the appropriate strength. Another possibility would be to destroy the stability of the other metastable phases and achieve the phase with minimal energy by a form of magnetic shaking, e.g. by the application of fluctuating fields of decreasing amplitude.

For magnetic storage applications, on the other hand, the stability of the dot configurations is advantageous, indeed, essential. Experimental observation of these dot arrays and transitions between their states may perhaps also be useful for the determination of the basic dot parameters, in particular the radius of the vortex core and its magnetic moment.

Last, but not least: these results are clearly not restricted to a dot lattice of the type considered here, but also apply directly to any square lattice of identical dipoles that are restricted to the two senses of normal orientation. They may also be relevant to the description of other uniaxial dipole-coupled systems of small particles, for example, thin films of granular magnets with easy axial anisotropy (shape or crystallographic) with a perpendicular easy axis and negligible exchange coupling between granules. Such properties are characteristic for thin films prepared by simultaneous evaporation of permalloy and silver with small enough concentrations of permalloy.<sup>20</sup>

## Acknowledgments

This work was supported in part by grant INTAS - 97 - 31311

\* Electronic address: bivanov@i.com.ua

<sup>1</sup> B. Hillebrands, C. Mathieu, C. Hartmann et al., J. Magn. Magn. Mater. **75**, 10 (1997).  
<sup>2</sup> C. Miramond, C. Fermon, F. Rousseaux et al., J. Magn. Magn. Mat. **165**, 500 (1997).  
<sup>3</sup> E.F. Wassermann, M. Thielen, S. Kirsch et al., J. Appl. Phys. **83**, 1753 (1998).  
<sup>4</sup> K. Runge, T. Nozaki, U. Okami et. al., J. Appl. Phys. **79**, 5075 (1996).  
<sup>5</sup> R.P. Cowburn, D.K. Koltsov, A. O. Adeyeye et al., Phys. Rev. Lett. **83**, 1042 (1999).  
<sup>6</sup> N.A. Usov and S.E. Peschany, J. Magn. Magn. Mater. **130**, 275 (1994). R.P. Cowburn and M.E. Welland, Phys. Rev. **B58**, 9217 (1998); R. P. Cowburn, A. O. Adeyeye, and M. E. Welland, Phys. Rev. Lett., **81**, 5415 (1998).  
<sup>7</sup> N.A. Usov and S.E. Peschany, J. Magn. Magn. Mater. **118**, L290 (1993).

<sup>8</sup> A. Fernandez and C. J. Cerjan, J. Appl. Phys. **87**, 1395 (2000).  
<sup>9</sup> Jing Shi, S. Tehrani and M. R. Scheinfein, Appl. Phys. Lett., **76**, 2588 (2000).  
<sup>10</sup> T. Pokhil, D. Song and J. Nowak, J. Appl. Phys. **87**, 6319 (2000).  
<sup>11</sup> V. Novosad, K. Yu. Guslienko, Y. Otani et al., MMM-Intermag Conference, paper EY-07, Proceedings (2001).  
<sup>12</sup> A. M. Kosevich, B. A. Ivanov, and A. S. Ko-valev, Phys. Rep. **194**, 117 (1990); V.G.Bar'yakhtar, B.A.Ivanov, Soliton thermodynamics of low-dimensional magnets. Sov.Sci.Rev. A. - Phys., Ed.by I. Khalatnikov, **16**, 1 (1992).  
<sup>13</sup> B. A. Ivanov, H.J. Schnitzer, F.G. Mertens and G.M. Wysin, Phys. Rev. **B58**, 84861 (1998).  
<sup>14</sup> K. Yu. Guslienko and A. N. Slavin, J. Appl. Phys. **87**, 6337 (2000).  
<sup>15</sup> B. A. Ivanov and D. D. Sheka, Sov. J. Low Temp., Phys.

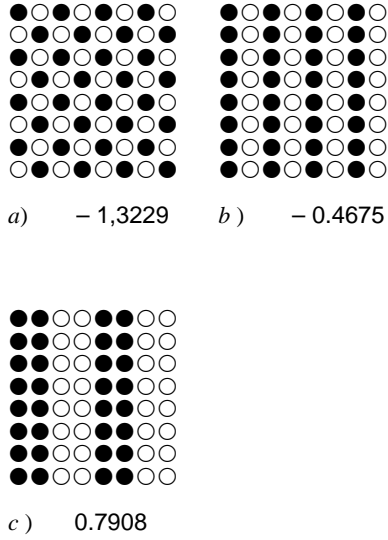


FIG. 1: Different antiferromagnetic states for a square magnetic dot lattice. The dipolar energies per dot of the lattices (in units of  $(\mu^2/a^3)$  - see text) have been found numerically and printed below each sketch. Open circles  $\circ$  denote the "up" dots with moments  $\vec{\mu} = \mu\hat{z}$ ; solid circles  $\bullet$  correspond to "down" dots with  $\vec{\mu} = -\mu\hat{z}$ .

- 21**, 1148 (1995).
- <sup>16</sup> Ar. Abanov, V. Kalatsky, V.L. Pokrovsky, and W.M. Saslow, Phys. Rev., **B51**,1023 (1995)
- <sup>17</sup> J. Arlett, J.P. Whitehead, A.B. MacIsaac, and K. De'Bell, Phys. Rev., **B54**, 3394(1996)
- <sup>18</sup> J.M. Luttinger and L. Tisza, Phys. Rev. **70**, 954, 1946.
- <sup>19</sup> P.I. Beloborodov, R.S. Gekht and V.A. Ignatchenko, Sov. Phys. - JETP **57**, 636 (1983).
- <sup>20</sup> D. Pod'yalovskii, A. Pogolrilyi, B. Ivanov, A. Kravits, C.S. Kim, JMMM **196-197**, 131 (1999).

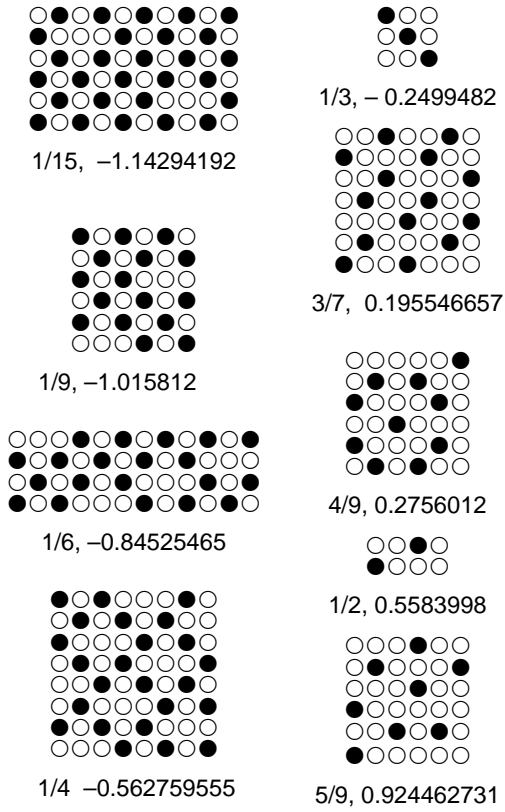


FIG. 2: Some lattice structures with intermediate values of  $m = \langle \mu_z \rangle / \mu$ ,  $0 < m \leq 5/9$ , and thought to have least dipolar energy for that value of  $m$ . The values of  $m$  and dipolar energy per dot of each structure (in units of  $\mu^2/a^3$ ) are printed below it.

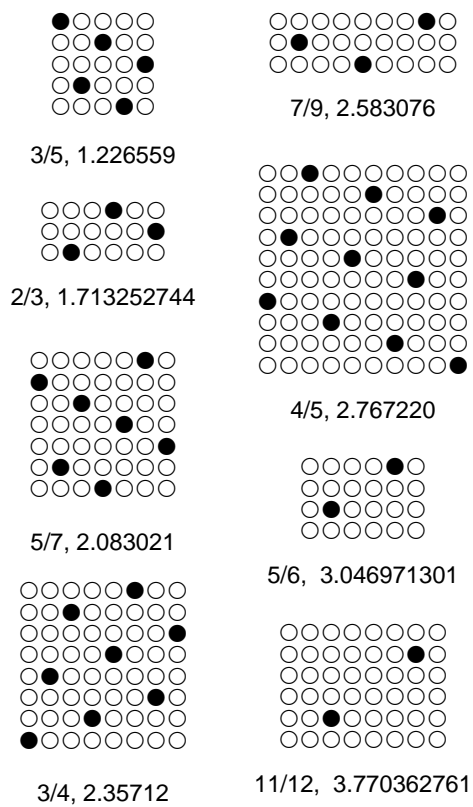


FIG. 3: As Fig.2, but for  $3/5 \leq m < 1$ .

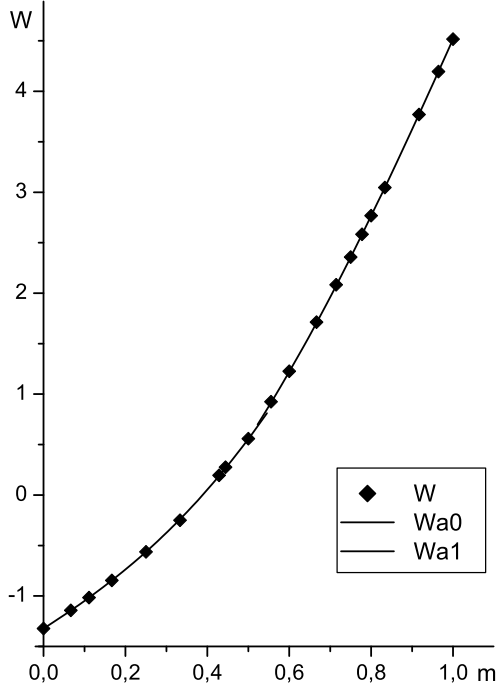


FIG. 4: Dependence of optimal lattice dipolar interaction energy per dot,  $W_m$ , on reduced lattice magnetization  $m$ . The points  $W$  represent values calculated for specific structures (as in Figs.2,3). Curves  $Wa1$  and  $Wa0$  represent the analytic asymptotic formulae in Eqs.(6), (8). (All energies are in units of  $\mu^2/a^3$ .)

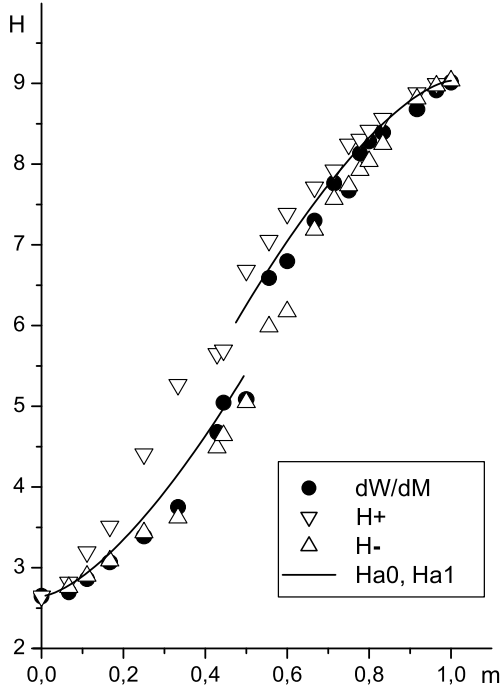


FIG. 5: An hysteretic magnetization curve for magnetic dot lattice. Solid circles labelled  $dW/dM$  represent approximate values of the equilibrium field  $H_m(m) = \mu^{-1}dW_m/dm$  derived numerically from the dipolar energies of the successive optimal lattice structures studied (see text). Threshold fields for reversing a *single* dot,  $H_-$  and  $H_+$ , are also shown. Curves Ha1 and Ha0 follow the analytic asymptotic formulae for  $H_m(m)$  in Eqs.(10, 11). (All fields are in units of  $\mu/a^3$ .)

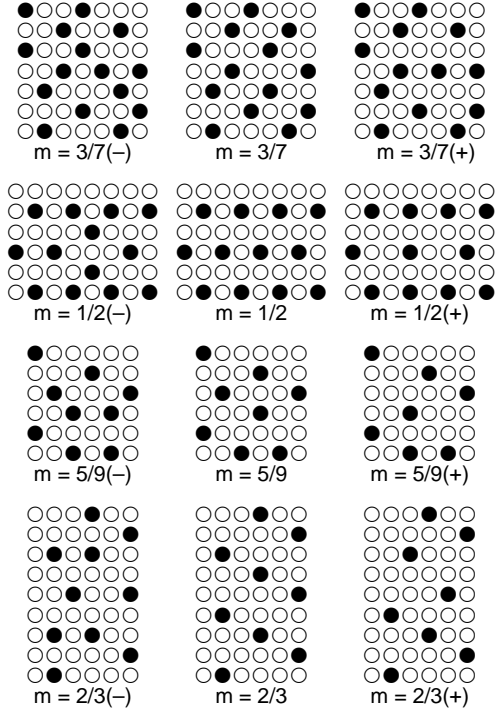


FIG. 6: Examples of optimal re-ordered structures after a single dot has been reversed in an optimal periodic lattice configuration of specific magnetization  $m$ . The central column shows the structures of individual cells in the initial periodic rectangular superlattice. Reversing a single up dot in a single such cell ("central" cell) and then rearranging to minimize the energy, alters the central cell structure to that in the left column. Similarly, the result of reversing a single down dot is shown in the right column. None of the other cells in the superlattice is altered.